JOURNAL OF GEOPHYSICAL RESEARCH, VOL. 95, NO. B9, PAGES 14,265–14,278, AUGUST 30, 1990

Resurfacing of the Martian Highlands in the Amenthes and Tyrrhena Region

ROBERT A. CRADDOCK AND TED A. MAXWELL

Center for Earth and Planetary Studies, National Air and Space Museum, Smithsonian Institution, Washington, D. C.

The southern cratered highlands of Mars contain a large population of flat-floored, rimless craters which have previously been interpreted to have formed by aeolian mantling or flood volcanism. Neither of these geologic processes accurately explains the observed morphology or the crater statistics. Geologic mapping in the Amenthes and Tyrrhena region indicates that craters with this morphology occur on undulating intercrater materials near the dichotomy boundary and on more rugged materials farther into the highlands containing numerous ancient valley networks. Cumulative size-frequency distribution curves indicate ages of $N(5) = 790$ (early to middle Noachian) and $N(5) = 540$ (middle Noachian) for the cratered plateau and cratered highland materials, respectively, opposite the observed stratigraphic relations. For crater diameters >16 km the population of impact craters is consistent with stratigraphy, but the population of smaller craters in the region indicates the importance of resurfacing. Superposed, fresh craters indicate a resurfacing event that ceased at $N(5) = 200–250$ (late Noachian to early Hesperian). Crater counts divided into 5° latitudinal bins show an increase in the number of craters between the 8- and 50-km-diameter range with increasing northerly latitudes, suggesting that the resurfacing was not a single event. Statistical modelling of an erosive event capable of removing the continuous ejecta deposits from the craters, eroding them to reduce the apparent diameter, and simultaneously burying smaller eroded craters explains both the morphology of the flat-floored, rimless craters, and their population distribution. Matching the slope of the modelled curves with that of the cratered highland materials suggests that up to 1400 m of erosion may have taken place in the highlands. Some of this eroded material probably remained locally, burying the smaller craters. Later stripping of this material indicated by exposed layering and inverted topography has exhumed the smaller craters in the cratered plateau material resulting in the apparent age discrepancy determined from crater counts. Up to 1.0 km of material may have been removed by this later erosive event to explain the low density of ancient valley networks in the cratered plateau materials.

INTRODUCTION

"Resurfacing" is a term used to describe any number of geologic processes responsible for modifying the surface of a planet. Volcanism [*Hartmann et al.*, 1981], impact cratering [*Hartmann*, 1971], fluvial processes [*Tanaka et al.*, 1988], aeolian deposition [*Wilhelms and Baldwin*, 1989], and periglacial processes [*Tanaka et al.*, 1988] have all been proposed to explain photogeologic observations and/or size-frequency variations of crater populations of the Martian surface. Our objective is to determine both the age of and the processes responsible for modification of the crater population along the dichotomy boundary of Mars. Such constraints are needed in order to determine accurately the geomorphic evolution of the Martian highlands, to bracket the age and origin of structural events occurring on the Martian dichotomy boundary, and to understand eventually the origin of the boundary itself. In this paper we concentrate on the Amenthes and Tyrrhena quadrangles in the eastern hemisphere of Mars because the boundary in this area is removed from the geologic influence of structures and young lava flows associated with the large Tharsis volcanoes, thus enabling relatively older geomorphic processes unique to the highlands to be investigated.

Amenthes (MC-14) and Mare Tyrrhenum (MC-22) are located at the southern edge of the Martian dichotomy boundary southwest of Elysium Mons, between longitude 225° and 270°W and −30° to 30° latitude. Since this study concentrates on the resurfacing processes defined by morphologic features in the highlands, only the southern portion of the Amenthes quadrangle was investigated (Figure 1). The surface of Hesperia Planum and similar age plains units (e.g., the Herschel basin floor) were not included because they represent relatively young resurfacing by volcanic extrusion, a process well-documented on several planets. The older surfaces of southern Amenthes and Tyrrhena are distinctly higher than the young plains units. South of Elysium Planitia, surface elevation rises approximately 2 km (topography from the *U.S. Geological Survey* [1989]) but does not become level until farther south into the highlands near latitude −10°. Elevations decrease southwest of latitude −30° due to the presence of the Hellas basin.

An old episode of highland resurfacing is illustrated by the occurrence of flat-floored, rimless craters that occur on materials ranging from rugged terrain to smooth plains. Both the etched nature of the intercrater surfaces and the shape of the crater size-frequency distribution curves imply erosional processes rather than only deposition of materials up to crater rim crests, as suggested by *Hartmann* [1971] and *Wilhelms and Baldwin* [1989]. However, some deposition must have taken place in order to account for the flat crater floors and deposits of smooth plains material that blanket more highly cratered, older terrain. These observations suggest a complicated series of resurfacing events, as well as a variety of processes. The results of these processes have a marked effect on the crater counts used to define the age of faulting [*Maxwell and McGill*, 1988] and on the amount of exposure of the oldest geologic units in the region [*Craddock and Maxwell*, 1989]. In particular, this paper addresses the timing of resurfacing represented by the population distribution curves of the flat-floored, rimless craters, the origin of this unique population, and the areal extent and thickness of

Paper number 90JB00833.

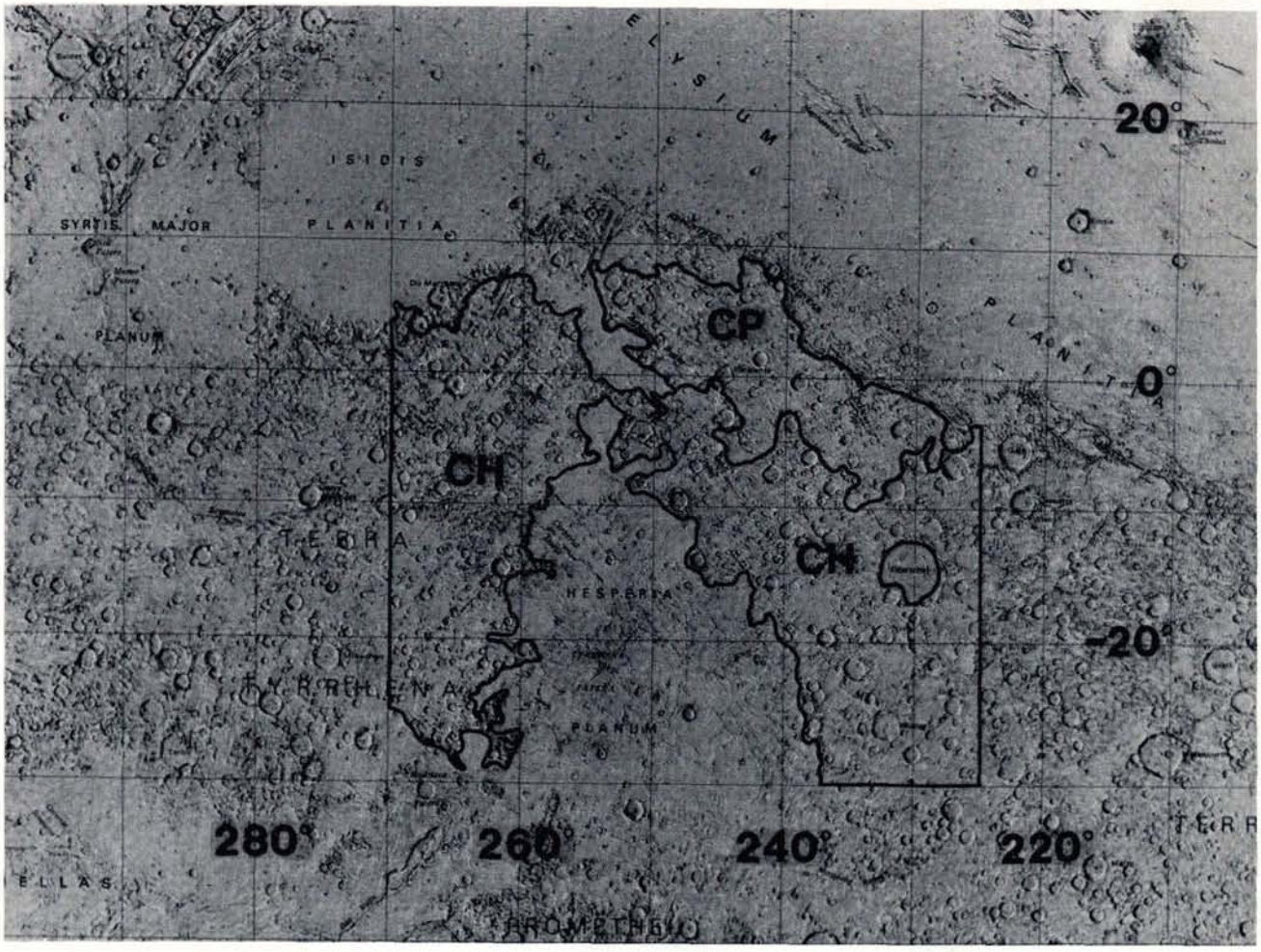

Fig. 1. Shaded relief map of the Amenthes and Tyrrhena region. Areas outlined show the location of the cratered plateau material (CP) and the cratered highland materials (CH). Base map is 1:15,000,000 shaded relief map of the eastern region of Mars [*U.S. Geological Survey*, 1985].

materials responsible for modifying the highland surface of this part of Mars.

Resurfacing Effects on Highland Crater Populations

The morphology and size distribution of Martian highland craters have been the subject of numerous studies. Observations made from Mariner spacecraft data showed that many of the craters in the Martian highlands were unlike those observed on the Moon [*Leighton et al.*, 1965]; Martian craters greater than 20 km in diameter were noticeably subdued, whereas smaller craters were lunarlike in their bowl-shaped appearance [*Opik*, 1966]. *Murray et al.* [1971] attributed the differences in crater morphology to periodic erosional events early in the history of Mars, and *Hartmann* [1971] suggested that the morphologic differences were due to deposition of aeolian materials generated by the cratering process. The change in slope of the highland crater population distribution at 50 km was interpreted by *Hartmann* [1973] to represent an early, intense erosional/depositional event, followed by an intermediate rate of erosion/deposition and the continued formation of impact craters. Alternatively, *Chapman and Jones* [1977] suggested that after the early, intense event, resurfacing suddenly stopped and the break in the slope of the crater population represents later crater formation. *Hartmann*'s [1973] model implies that early resurfacing processes tapered off gradually with time, while *Chapman and Jones*' [1977] model suggests that the resurfacing processes were catastrophically shut off. Without the independent interpretation of crater morphology or stratigraphic assignment of surface ages, the number and types of resurfacing events were thus difficult to interpret based on population distributions alone.

In defining a "standard Mars crater population distribution", *Neukum and Hiller* [1981] made the ad hoc assumption that target effects were negligible in producing bends in the population distribution curve and interpreted each break in slope with a discrete resurfacing event. By subtracting each continuous population distribution that matches the standard production curve, several surface ages can be determined from a single crater count. For the eastern hemisphere, this method enabled *McGill* [1987], *Frey et al.* [1988*a*, *b*], *Maxwell and McGill* [1988], and *Frey and Grant* [1989] to date several episodes of resurfacing which may have taken place along parts of the crustal dichotomy boundary. For large areas of Mars, recent work by *Tanaka*

et al. [1988] suggests that global resurfacing has gradually decreased with time and involved a variety of geologic processes. However, the nature and the timing of early resurfacing events in the southern cratered highlands are not yet fully understood.

In the Amenthes and Tyrrhena region, *Frey et al.* [1988*a*] found three separable Lunae Planum age (early Hesperian) resurfacing events and determined that a major resurfacing event ceased in the Amenthes highlands at $N(1) = 86{,}000$ ($N(5) = 1858$, or early to middle Noachian). Although *Frey et al.* [1988*a*] determined a relative timing of resurfacing events and the related efficiency of the process, the mechanism for the resurfacing is mentioned only as burial. The relative timing of the resurfacing events is also model dependent; the *Neukum and Hiller* [1981] production curve is not a straight-line power law production curve and includes crater counts of regions that have undergone resurfacing. This results in age dates determined from branches in the cumulative frequency curves that may be too young.

Investigations by *Maxwell and McGill* [1988] in the Amenthes region confirmed the model dependency of subtracting production curves from cumulative curves of a given area or geologic unit. They also recognized that the cratered plateau material east of Isidis Planitia contains two crater populations resulting from a resurfacing event that stripped the rims of the older population by the end of the late Noachian ($N(5) = 230$). The termination of the resurfacing event also coincides with the age of the ridged plains materials located north of the boundary. Independently, *Wilhelms and Baldwin* [1989] determined the relative ages of both crater populations in the same region, confirming the late Noachian/early Hesperian time of resurfacing in the region.

Apart from size variations in the crater population, several lines of evidence from surface morphology also indicate a complex history of resurfacing: (1) The distinct population of rimless craters recognized by *Maxwell and McGill* [1988] and *Wilhelms and Baldwin* [1989] suggests either a unique characteristic of the impacted material suddenly changed, or more likely, a complex series of erosional and sedimentary processes as will be discussed later; (2) numerous dendritic valley networks occur on cratered plateau material and on the rims of large impact basins, and in several cases appear to terminate and reappear as if intervening parts of channels have been buried or eroded; (3) a combination of the morphology of small landforms and crater statistics indicated to *Grizzaffi and Schultz* [1989] that a 150-m to 2-km thick transient air fall deposit was interlain with ice in Isidis Planitia and was subsequently removed, resulting in formation of arcuate ridges and mounds; and (4) stratigraphic relations of cratered terrain and overlying plains deposits indicate at least two episodes of plains emplacement: an early intercrater plains that occupies areas between rugged highlands and exhibits ridges of probable tectonic origin [*Watters*, 1988], and a less cratered, smooth plains deposit that occupies areas adjacent to the dichotomy boundary. These smooth plains are the same age as young smooth plains material in the northern plains [*Maxwell and McGill*, 1988].

Although selected features and stratigraphic relations individually can be explained by "normal" planetary resurfacing by volcanic and aeolian deposits, we believe that the combination of the unique population of rimless craters, the association with regional depositional centers downslope from the Amenthes/Tyrrhena region, and the presence of old, partially destroyed drainage networks all suggest an enhanced period of surface erosion of the cratered highlands in this region. We present below a discussion of the timing of the erosional and depositional history based on the populations of impact craters and use the population distribution along with surface morphology to determine the mechanism of resurfacing in the region.

TIMING OF RESURFACING EVENTS

Two highland units containing rimless craters were recognized in the Amenthes and Tyrrhena regions, cratered highland materials and cratered plateau materials, which correspond to the hilly and cratered materials and the cratered plateau materials of *Scott and Carr* [1978]. Both units are subdivisions of the dissected plateau sequence of *Greeley and Guest* [1987]. The cratered highland materials (Figure 2) have a population of rimless craters, but intercrater materials are rugged and deeply etched and contain numerous ancient valley networks. The cratered plateau materials (Figure 3) typically form a relatively smooth, gently undulating intercrater surface with limited occurrences of ancient valley networks. Although very extensive, Hesperia Planum, associated Tyrrhena Patera deposits, and similar appearing materials (e.g., floor materials of Herschel basin) were not included in this study because of their relatively young age [*Greeley and Guest*, 1987; *Tanaka et al.*, 1988] and the lack of rimless craters.

Populations of both rimless and fresh (superposed) craters for both units were counted and normalized to measure the crater size-frequency distribution of the surfaces. This process has been reviewed by *Neukum and Wise* [1976], *Neukum and Hiller* [1981], and *Tanaka* [1986]; crater diameters in a given area are counted and the frequency is normalized to some unit area, typically 10^6 km^2 [*Tanaka*, 1986]. The cumulative frequency is plotted on a logarithmic scale and the number of craters greater than a given diameter [$N(D)$] is either read directly from the plot [*Tanaka*, 1986], or a production curve is fitted to the data [*Neukum and Wise*, 1976; *Neukum and Hiller*, 1981]. Previous work has shown that the determination of resurfacing ages is dependent on which production curve is used [*Maxwell and McGill*, 1988]. The production curve of *Neukum* [1983] incorporates additional bends in the curve not present in the *Neukum and Hiller* [1981] curve, which may be the result of including areas that have undergone resurfacing in the generation of the production curve. For this reason, the resurfacing ages in this study were determined directly as in *Tanaka*'s [1986] method.

Although a larger sampling area for the cratered plateau materials was used than in previous work (494,440 km^2 versus 173,200 km^2 of *Maxwell and McGill* [1988]), the size-frequency distribution remained basically the same (Figure 4; compare with Figure 5 of *Maxwell and McGill* [1988]). The $N(5)$ age of this surface is equal to 790 (early to middle Noachian), with a resurfacing age of $N(5) = 250$ (late Noachian) as represented by separate counts of fresh, or superposed craters. In contrast, the age of the cratered highland materials (Figure 5) is $N(5) = 540$ (approximately middle Noachian) with a resurfacing age of $N(5) = 200$ (late Noachian to early Hesperian). Based on crater counts alone, the cratered plateau material appears to be older than the

Fig. 2. Flat-floored, rimless craters in the cratered highland materials. The etched nature of the intercrater plains suggests erosion of the continuous ejecta deposit as opposed to deposition up to the rim crest. North is to the top. (Viking orbiter frames 381S81-83, 629A22, and 629A24 in MC-22 NE.)

cratered highland material. However, the frequency distribution curves for these two units cross at 16 km, and only those craters greater than 25 km indicate age relations consistent with stratigraphic observations, in which cratered highland materials have a greater observed density than the cratered plateau materials.

Such age relationships may result from preferential stripping of craters <16 km in diameter from cratered highland material, or lack of retention of those craters because of the rugged relief and possible highly fractured surface materials. The cratered plateau materials may retain smaller craters because of their relatively low relief and incorporation of small patches of intercrater plains that are included in that unit. Although the age of the unmodified crater population in the cratered highland materials is slightly younger than that of the crater plateau materials ($N(5) = 200$ versus $N(5) = 250$; both approximately late Noachian), they are essentially equivalent to each other, and the fresh crater population that they represent contributes little to the total crater age contrast between the units.

The age relationships are consistent with observations made by *Dimitriou* [1989] in the highlands materials of the Ismenius Lacus quadrangle. The geologic unit away from the boundary in the Ismenius Lacus region has an age similar to the cratered highland material in the Amenthes/Tyrrhena region, and the Ismenius Lacus near-boundary unit also has an age close to that of the cratered plateau material in the Amenthes/Tyrrhena region (A. M. Dimitriou, personal communication, 1989).

To determine whether the timing of the resurfacing was related to the dichotomy boundary or other possible geologic events (e.g., the Isidis basin air-fall deposit of *Grizzaffi and Schultz* [1989]), counts on the cratered plateau surface were divided into 5° latitude bins. These frequency distributions (Figure 6) suggest an increase in the age of resurfacing with increasing northerly latitude (toward the dichotomy boundary), and the variation is evident in the same diameter range (8 and 50 km), suggesting that the physical properties of the substrate do not have an effect on the population variations observed. If resurfacing was a single process, these data imply a time transgression such that the surface nearest the dichotomy boundary became stable first, followed by cratered plateau surfaces at successive southerly latitudes. Timing sequences analogous to this, but in another direction, have been noted by *Frey et al.* [1988*a*], in which cessation of resurfacing within the younger smooth plains and fretted terrain was progressively younger west of Isidis, toward more northerly latitudes.

The variation of resurfacing age with latitude observed here is intriguing but is based on only minor deviations in the curves and is not apparent in the small (<8 km) crater population. Based on the data collected for Amenthes and

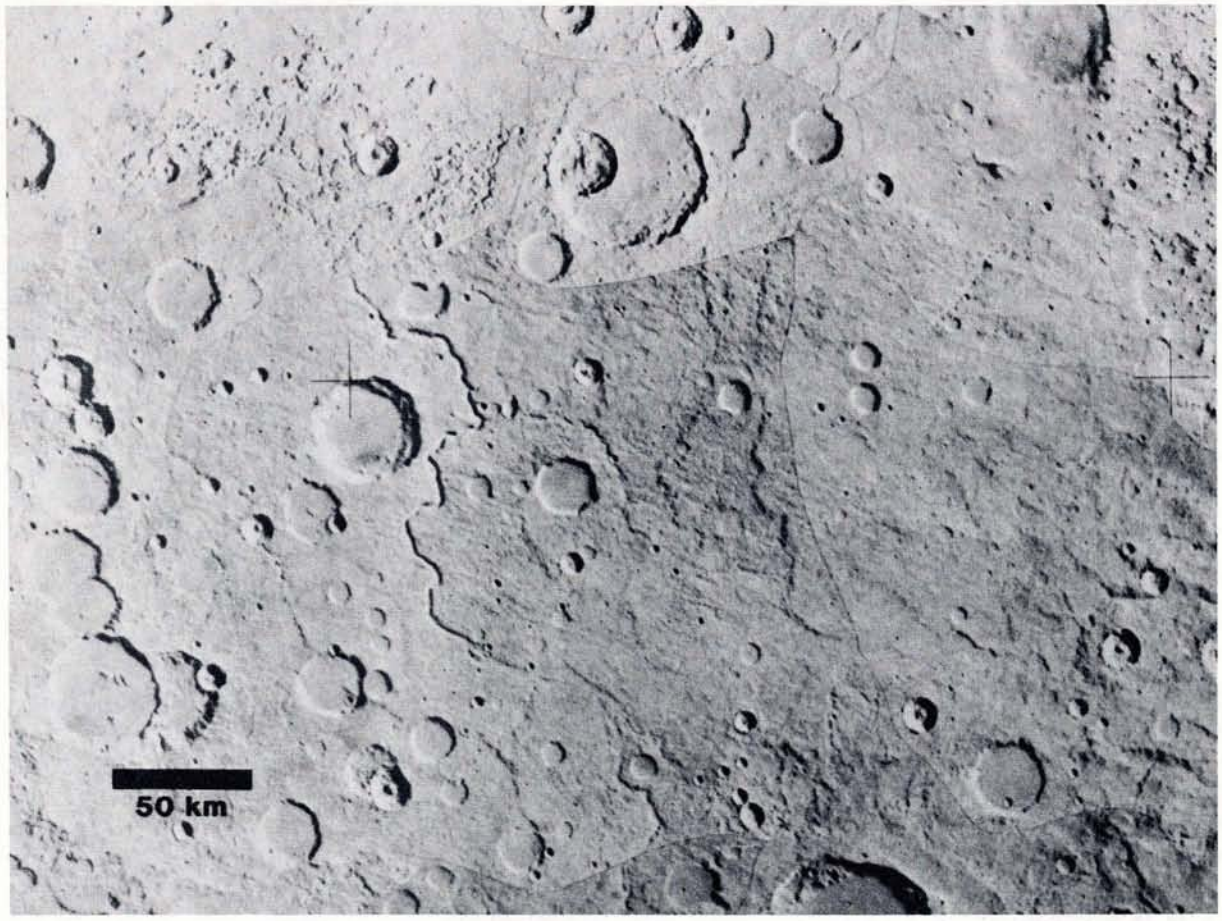

Fig. 3. Flat-floored, rimless craters in the cratered plateau materials. Note the smooth, gently undulating nature of the intercrater plains. North is to the top. (Viking orbiter frames 381S41-46 in MC-14 SE.)

Tyrrhena, we cannot tell whether these age variations are related to latitude (which could imply climatic effects in the resurfacing process) or to distance from the dichotomy boundary (implying structural modification or topographic effects on the surfaces).

Resurfacing Mechanisms

Of all of the geologic processes active presently or in the past on Mars, only a few seem likely to have had the capability to remove or obscure the rims of large (>10-km diameter) craters. These processes include aeolian erosion or deposition, volcanism, and fluvial erosion and deposition. Other processes such as periglacial activity are not considered here because evidence for such processes has not been recognized in the Amenthes and Tyrrhena regions. Amenthes and Tyrrhena are also located between ±30° latitude, away from occurrences of terrain softening observed by *Squyres and Carr* [1986] and *Squyres* [1989] at higher and lower latitudes. Terrain softening as a method for modifying craters can be further ruled out by the absence of downhill flow of materials and the existence of rugged, etched intercrater plains. Using some published experimental data and quantitative crater parameters, we have modelled aeolian, volcanic, and fluvial processes in terms of their effect and efficiency in modifying crater morphology and population characteristics.

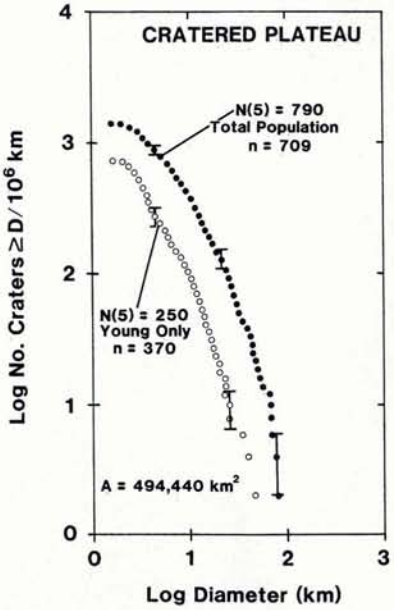

Fig. 4. Cumulative crater frequency plots of the cratered plateau materials. Change in slope at about 10 km indicates a resurfacing event which reduced the number of small craters. Photogeologic observations indicate that larger craters were also affected by this event.

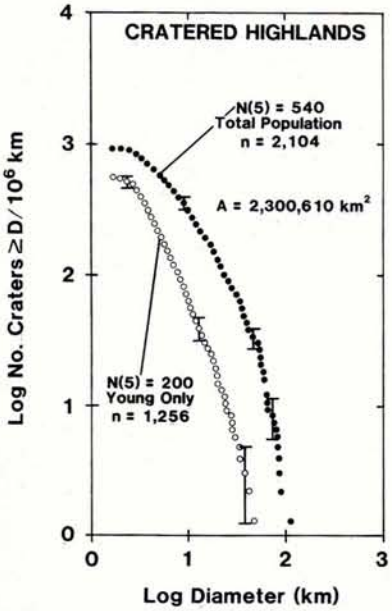

Fig. 5. Cumulative crater frequency plots of the cratered highland materials. Note that the $N(5)$ age for both total and young (i.e., superimposed) curves is less than the $N(5)$ age of the cratered plateau materials.

Aeolian Resurfacing

Vast portions of the Martian surface are thought to be covered by aeolian material [*Soderblom et al.*, 1973; *Carr et al.*, 1973; *Scott and Carr*, 1978]. The bendover in the Martian crater production curve has been explained by the deposition of aeolian material [*Hartmann*, 1971], and burial up to the crater rim crest by aeolian material has been proposed to explain the morphology of the flat-floored, rimless craters in the Amenthes and Tyrrhena regions [*Wilhelms and Baldwin*, 1989; *Moore*, this issue]. However, aeolian deposition does not explain the observed diameter range of rimless craters, nor does burial alone match the morphology of a range of crater diameters. Below we present a simple model for the effect of burial on crater morphology and size-frequency relations. The effects of aeolian erosion are discussed later.

One end-member model of a cratered surface that undergoes burial by aeolian materials is illustrated in Figure 7. At first, only small craters are completely buried or obscured, with larger crater rims, floors, and flanks being partially covered. With continued burial or with later depositional events the rims of larger craters are buried to a greater depth. The depth of material on top of the rim is dependent upon the cohesion of deposited material, the angle of internal friction of the material, the topographic slopes inside and outside of the rim crest (and/or the width of the rim crest), and to a minor extent, the gravity of the planet [*Klein and White*, 1988]. Under Martian conditions it seems reasonable to assume that at least some material would slump into the crater interior and around the outer rim, but some material would remain in situ and subdue irregularities in the rim crest. The important point is that material is not deposited up to the rim crest and on the floor but is deposited on the flanks and on rim crest as well. This results in a crater that is subdued and eventually buried, but not a crater without a raised rim and a steep scarp separating the rim from the flat-floor, as observed.

Experimental modelling by *Zimbelman and Greeley* [1981] and Viking photographic data in Vastitas Borealis (Figure 8) illustrate the sequence of events modelled in Figure 7 and show that with continued deposition of materials the small craters disappear and the larger craters become more subdued. With time, even the larger craters become buried. Although the rim morphology changes, the diameter of recognizable craters remains the same as that of unmodified craters.

A cumulative crater frequency curve showing the effect on the crater population after several depositional events is shown in Figure 9. The curve at t_1 represents a crater distribution curve based upon *Neukum and Hiller* [1981] cumulative size-frequency data for large Martian craters and extrapolated to smaller crater diameters. At t_2 the smaller craters have been buried, and the larger craters have been blanketed by aeolian material. At t_3, progressively larger craters have been buried and with the continued formation of craters, the cumulative curve may take on the appearance of the standard Mars production curve. Although this resurfacing process is one possible explanation for irregularities in the global production curve [*Hartmann*, 1971, 1973], the results of this process do not match the change in slope of the cumulative curves observed locally (Figures 4 and 5) nor does it explain the lack of raised rim, relatively steep interior scarp, or flat-floor of the highland craters.

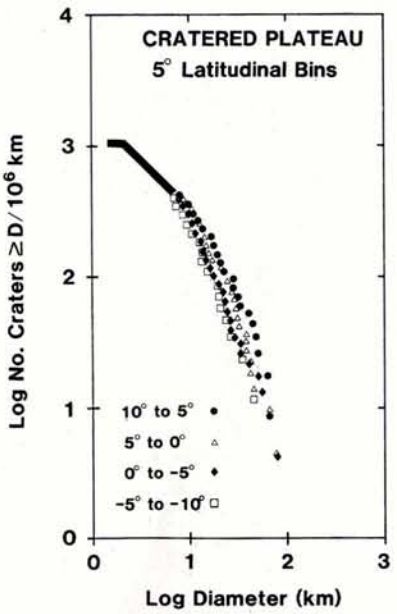

Fig. 6. Crater frequencies for the cratered plateau materials divided into 5° latitudinal bins. The number of craters between 8- and 50-km-diameter increases with increasing southerly latitudes, suggesting a time transgressive event in toward the highlands. Solid line indicates overlap between bins.

Volcanic Resurfacing

As much as 60% of the surface of Mars may be covered by volcanic material [*Greeley and Spudis*, 1981], leaving little doubt as to the importance of volcanism as a resurfacing process. The role of volcanic resurfacing in the Martian cratered highlands is less clear however. Volcanic materials

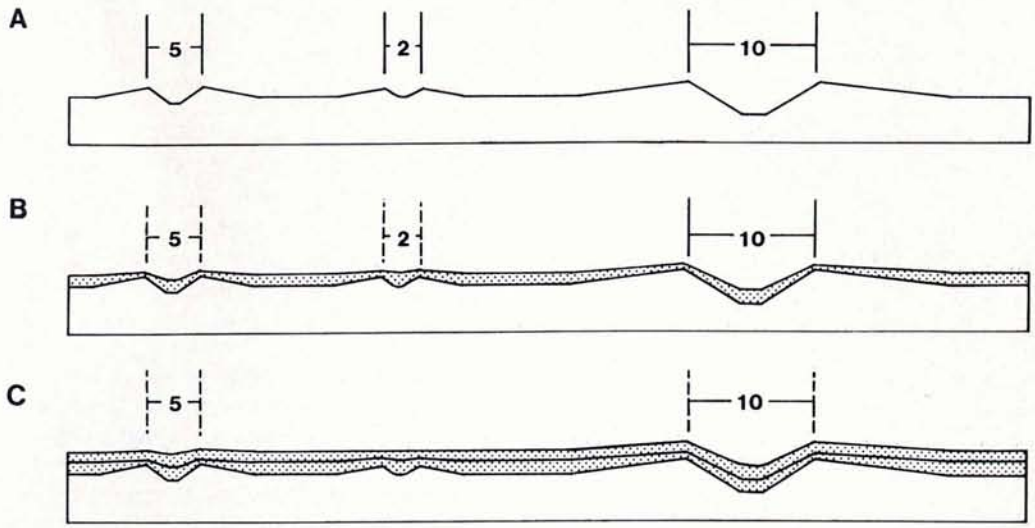

Fig. 7. Sequence of events during aeolian resurfacing based on experimental modelling by *Zimbelman and Greeley* [1981]. (*a*) Surface before aeolian blanket. (*b*) Smaller craters become almost completely buried while larger craters become more obscured after first deposit. (*c*) Smaller craters become completely buried. Larger craters become obscured but continue to have recognizable rims.

in most of the southern hemisphere of Mars are defined by their characteristic smooth surfaces and by the presence of wrinkle ridges [*Greeley and Spudis*, 1981; *Scott and Tanaka*, 1986; *Greeley and Guest*, 1987], which have traditionally been thought to represent compressional folding/faulting in basalt layers [*Wise et al.*, 1979; *Watters and Maxwell*, 1983, 1986; *Plescia and Golombek*, 1986]. These observations are not completely indicative of plains-type volcanism, and

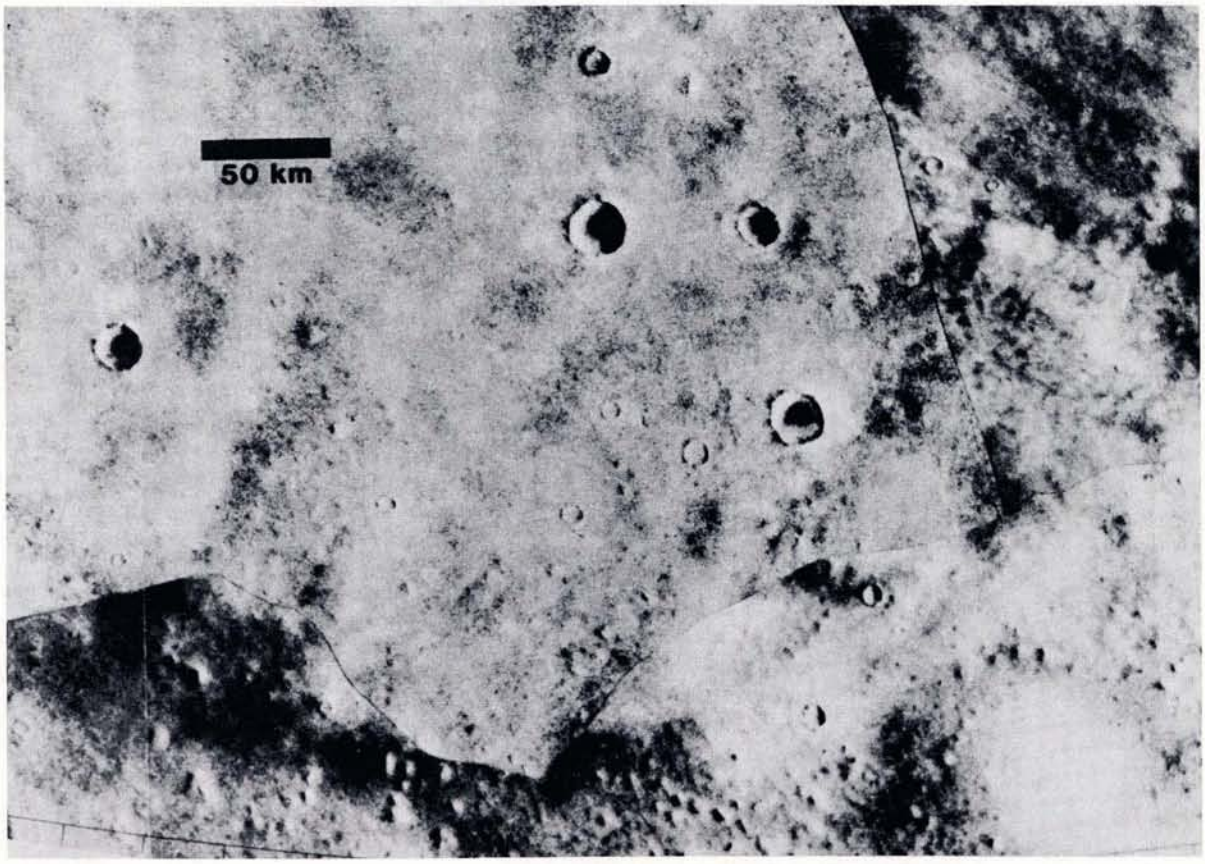

Fig. 8. Photograph of the Vastitas Borealis region showing burial and obscuration of craters by north polar aeolian materials. Note that crater rims remain visible, unlike the rimless craters in the southern highlands. North is to the top. (Viking orbiter frames 815A03-06 in quadrangle MC-1 F.)

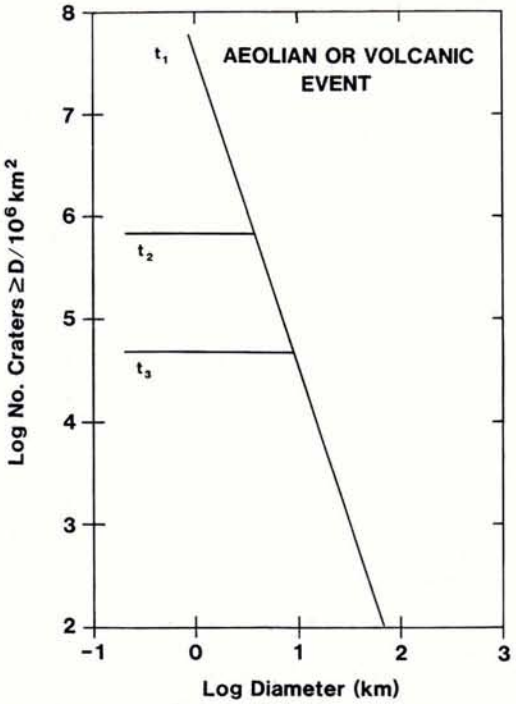

Fig. 9. Model cumulative crater frequency plots of aeolian or volcanic resurfacing events. With increasing intervals of times (t_1 to t_3) larger craters become less numerous due to burial. The important difference between the two processes is the effect on the crater rim morphology (compare Figure 8 with Figure 10).

alternative explanations such as localized extrusion or folding of sedimentary layers are possible [*Watters*, 1988].

Although *Cruikshank et al.* [1973] suggest that a rimless crater could occasionally be formed during mare emplacement on the Moon, the likelihood of the rimless crater population in the Amenthes and Tyrrhena regions resulting from volcanic resurfacing is poor despite the close proximity to Tyrrhena Patera. One or several volcanic resurfacing events producing the diameter range of rimless craters observed without producing any of the typical, partially flooded impact craters (Figure 10) is highly unlikely. In addition, no flow fronts, wrinkle ridges, or similar volcanic-related morphologic features are observed on the highland materials containing the rimless craters. Figure 11 illustrates the sequence of events associated with mare flooding or volcanic resurfacing. At first, small craters are flooded and, depending on the size, may be completely buried or remain as subtle "ghosts" (Figure 10). The crests of larger impact craters are not subdued, as in the case of aeolian mantling, but remain sharp with the outer slopes only partially covered. With time, increasingly larger crater rims are breached by the deposit, and flooding of the interior occurs. The resulting cumulative curve appears identical to the curve observed for aeolian mantling (Figure 9), since the apparent diameter as measured from orbital images would be the same. Morphologically, the craters would appear much different from those blanketed by air fall or affected by erosion (see below).

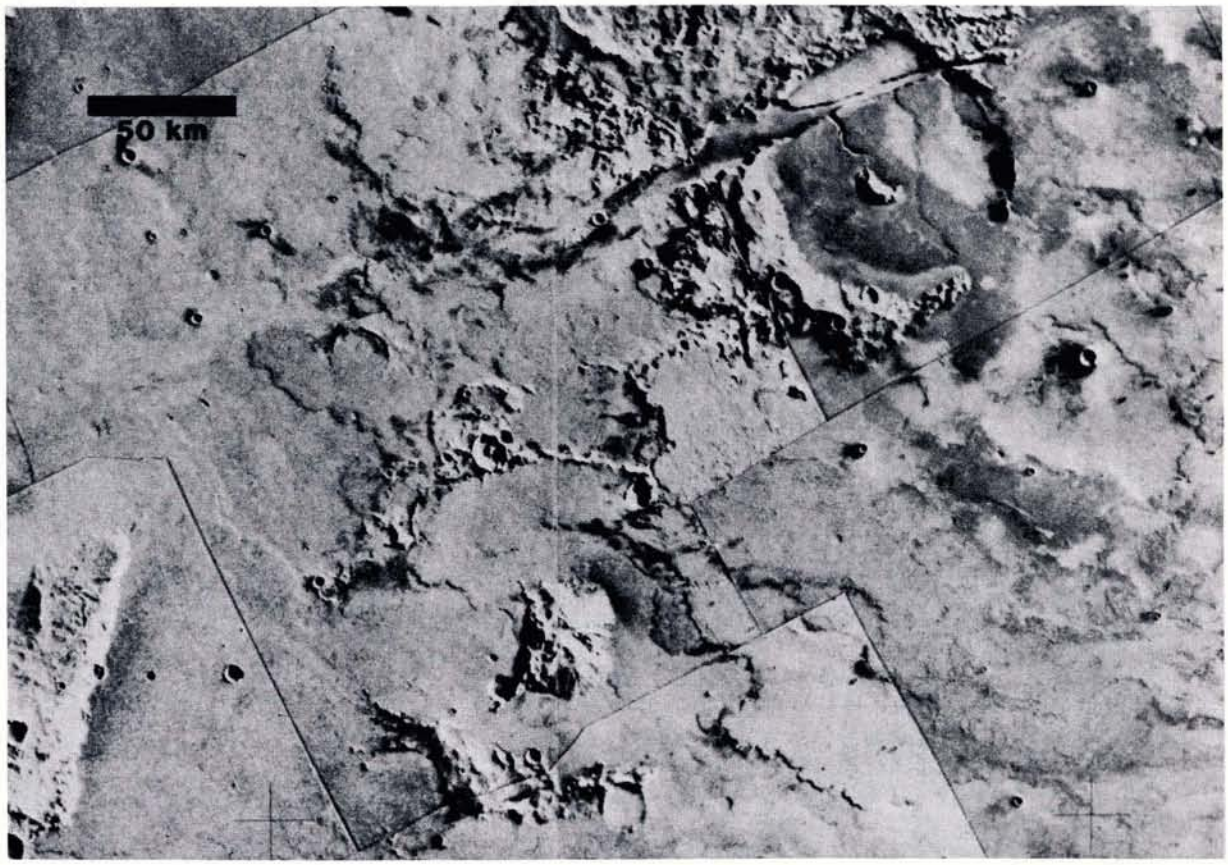

Fig. 10. Large, flooded impact craters in Daedalia Planum. Note the sharp crater rims, unlike the crater rims obscured by aeolian mantling in Vastitas Borealis (Figure 8). North is to the top. (Viking orbiter frames 639A11-14, 639A16, 639A35, and 639A37 in MC-16 SE.)

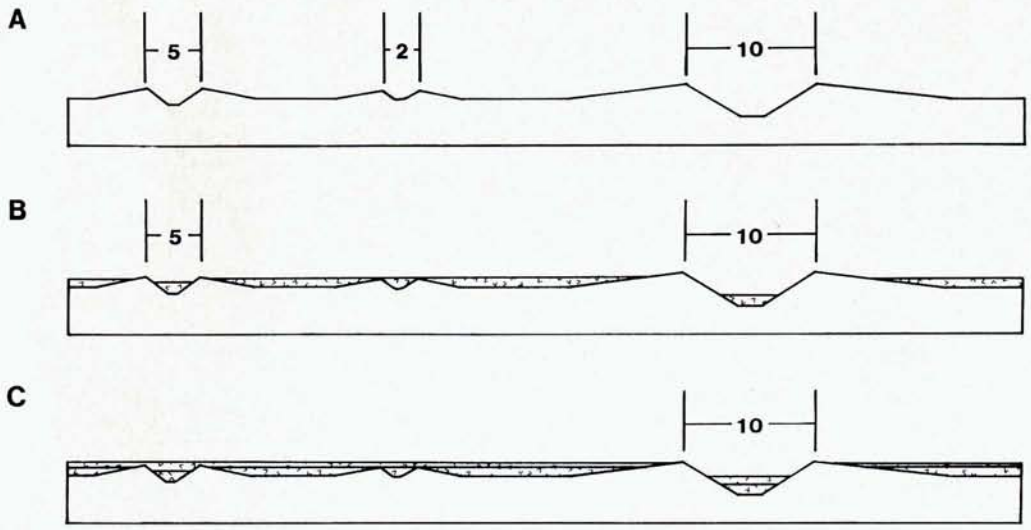

Fig. 11. Sequence of events showing volcanic flooding. (*a*) Preplains emplacement surface. (*b*) Material buries 2-km-diameter craters and encroaches on the ejecta deposits of the larger ones. (*c*) A 5-km-diameter crater is covered. Material breaches 10-km-diameter crater rim and begins to infill crater floor, further encroaching on the crater ejecta. The 5-km-diameter crater rim protudes as a "ghost" from the surrounding deposit.

Fluvial Resurfacing

A variety of landforms on Mars have been attributed to processes involving the interaction of ground ice and/or its release from the subsurface. These include outflow channels, which may have been formed by the catastrophic release of water [*Milton*, 1973; *Baker and Milton*, 1974; *Sharp and Malin*, 1975]; rampart craters, which may have formed by entrained gases caused by impact melting of ground ice [*Carr et al.*, 1977]; and patterned ground, which may have formed by the removal of ground ice at high latitudes [*Lucchitta et al.*, 1986]. In the highlands of Amenthes and Tyrrhena, valley networks [*Sharp and Malin*, 1975] dissect most of the intercrater plains and occasionally occur on the external slopes of large craters. Because of the dendritic pattern of the valley networks, *Masursky* [1973] and *Masursky et al.* [1977] have suggested that they are the result of rainfall runoff. Alternatively, the valleys may be the result of ground ice/water sapping [*Sharp*, 1973; *Sharp and Malin*, 1975; *Pieri*, 1976, 1980]. *Tanaka* [1986] determined that the valleys formed mostly during the middle to late Noachian and feed into smooth, late Noachian highland materials, consistent with the age of resurfacing determined for the Amenthes and Tyrrhena region.

In addition to the consistent age relationships between the peak time of channel formation and the age represented by rimless craters, the unique morphology of the flat-floored, rimless craters is suggestive of an erosional origin for several reasons. Such craters occur over a wide range of diameters: 2–50 km in the Amenthes/Tyrrhena region. Such a range is inconsistent with simple burial in which small craters up to some diameter cutoff point should not be present at all. Simple burial followed by erosion and exhumation of old craters would not result in the unique morphology observed. Where such exhumation has occurred on Mars, the rims of the buried craters emerge intact following removal of the overburden (see Viking orbiter frame 462S15; latitude 2.4°, longitude 140.5°). If extensive erosion due primarily to aeolian deflation were the cause of this crater population, we would expect crater frequency curves to match those under conditions of simple burial because of the long-distance transport of wind-eroded material.

For these reasons and the lack of simple aeolian or volcanic burial mechanisms to explain the morphology and population characteristics in the Amenthes/Tyrrhena region, we believe that these highlands have been subjected to an early intense period of fluvial erosion that progressively eroded larger and larger craters while depositing the material in both local and distant depositional centers. Such a process was likely aided by aeolian erosion of unconsolidated material originally weakened by fluvial reworking and deposition. Assuming that the rimless crater population represents some type of erosional mechanism, we developed a quantitative model that progressively erodes larger craters with time, while burying small craters with the eroded sediments.

Erosional Effects on Craters

Using morphometric parameters for Martian craters developed by *Pike and Davis* [1984], the rim height, crater diameter at ground level (i.e., rimless crater diameter), depth, and floor width were determined for a range of crater diameters between 2 and 50 km (Table 1). Measurements for the 2- to 10-km-diameter craters were determined by the equations for simple, bowl-shaped craters. Average interior slopes were determined using an equation developed by *Wood and Andersson* [1978] for lunar craters, which we have applied to fresh Martian craters in the absence of detailed topography:

$$\tan S = 2d/(D - D_f) \quad (1)$$

where S is the average interior slope; D_f is equal to 0 when the equation is applied to simple craters.

The volume of the continuous ejecta was then determined using

$$V = \pi[(1.5D + 0.5D_a)/2]h(1.5D - 0.5D_a) \quad (2)$$

assuming that the extent of the deposit extended for one crater diameter away from the rim crest. Using these data

TABLE 1. Martian Fresh Crater Parameters

Diameter D, km	Apparent Diameter D_a, km	Rim Height h, km	Depth d, km	Floor Width D_{fc}, km	Ejecta Volume V, km^3
2.0	1.63	0.074	0.390	NA	0.975
5.0	4.26	0.829	1.010	NA	19.17
10.0	8.41	0.354	2.069	NA	115.56
20.0	17.25	0.314	1.390	9.21	405.80
30.0	26.27	0.381	1.720	15.22	1105.09
40.0	35.40	0.437	1.980	21.73	2249.30
50.0	44.61	0.485	2.220	28.66	3893.80

Representative crater parameters are based on the work by *Pike and Davis* [1984], for simple (subscript s) and complex (subscript c) craters. Rim height h was determined from equation (T1) $h_s = 0.038D_s^{0.969}$ and equation (T2) $h_c = 0.076D_c^{0.474}$. The crater diameter at ground level (D_a) or the apparent diameter after removal of the ejecta is equation (T3) $D_{as} = 0.792D_s^{1.045}$ and equation (T4) $D_{ac} = 0.722D_c^{1.037}$. The crater depth d is equation (T5) $d_s = 0.190D_s^{1.037}$ and equation (T6) $d_c = 0.309D_c^{0.504}$. The floor diameter D_{fc} for craters greater than 10 km in diameter is equation (T7) $D_{fc} = 0.225\ D_c^{1.239}$.

(Table 1), the effects of crater erosion on population curves was determined.

For discussion purposes, we refer to the magnitude of an erosional event relative to the size of the crater which would have its rim and ejecta completely eroded to a precrater surface level. Thus, for a "2-km erosional event" the amount of material removed from any size crater is equal to the crater ejecta volume of a 2-km-diameter crater (Figure 12). Although backwasting and slope retreat are also processes which decrease the amount of crater rim material, they do not account for the relatively sharp interior scarp of the flat-floored, rimless craters. Table 2 includes crater frequencies determined from our modelled curve (Figure 9) and from the global production curve of *Neukum* [1983] fitted to the total crater population of the cratered highland materials. Cumulative volumes represent the total amount of material eroded from craters smaller than the given diameter "event." Given a 50-km erosional event, data from Table 2 indicate that a deposit between 750 and 2600 m thick may be emplaced over a (normalized) surface area of 10^6 km^2.

The values determined from our modelled curve represent upper limits to the total possible volume, and the amount determined from the *Neukum* [1983] curve represents a reasonable lower limit (Figure 9), as this curve may incorporate counts from resurfaced areas on Mars. The significance of a specific size event is that all of the continuous crater ejecta is eroded from that diameter crater, leaving a rimless crater whose apparent diameter can be determined by equation (T2) in Table 1.

The change in volume resulting from erosion of larger craters also results in a decrease in rim height, which in turn reduces the diameter of the crater by

$$D_e = D_a + 2[(V - V_e)/\tan S\pi(1.125D^2 - 0.125D_a^2)] \qquad (3)$$

where D_e is the diameter of the eroded crater and V_e is the amount of material eroded, equal to the ejecta volume V of the crater diameter associated with the erosional event.

At larger diameter erosional events, smaller craters (now rimless from the preceding smaller diameter erosional event) continue to be eroded, decreasing the apparent crater diam-

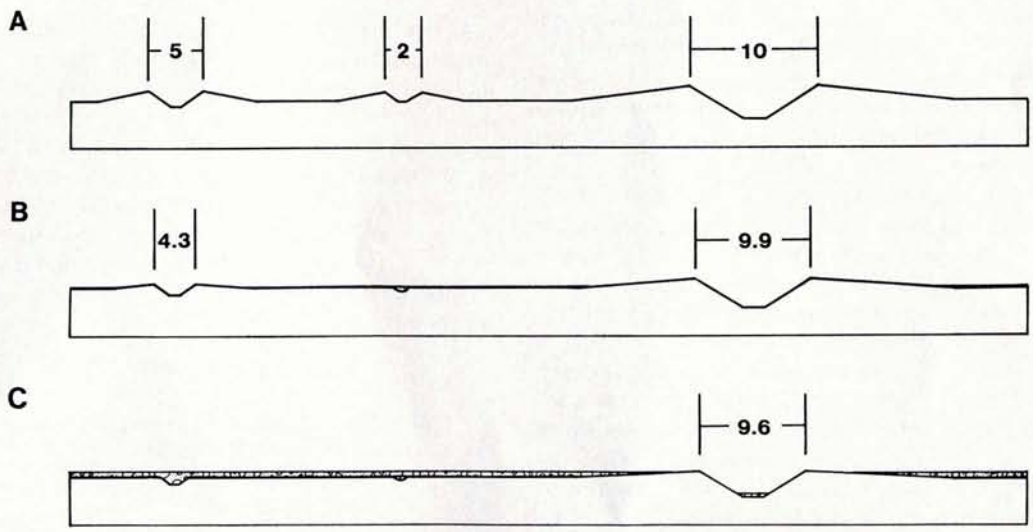

Fig. 12. Sequence of events involving erosion and deposition. (*a*) Surface before erosional event. (*b*) Sequence of events showing resurfacing during a 2-km-diameter erosional event. Material removed from larger craters results in a corresponding reduction in apparent crater diameter. (*c*) Sequence of events showing resurfacing during a 5-km-diameter event. In both Figures 12*b* and 12*c*, eroded materials bury smaller craters.

TABLE 2*a*. Modelled Crater Frequencies and Associated Volumes

Diameter, km	Frequency From Modelled Curve	Volume, km^3	Cumulative Volumes, km^3
2.0	600,000	585,000	585,000
5.0	40,000	766,800	1,351,800
10.0	4,500	520,020	1,871,820
20.0	600	243,480	2,115,300
30.0	180	198,916	2,314,216
40.0	70	157,451	2,471,667
50.0	28	109,026	2,580,693

Based on extrapolation of *Neukum and Hiller's* [1981] production curve from large (30- to 100-km-diameter) crater population to smaller craters; see Figure 9.

eter by both stripping of the surrounding terrain and infilling of the crater (Figure 12). *Maxwell and McGill* [1988] suggested that between 300 and 600 m of material had been eroded from the highlands based on the rim height of the maximum diameter of flat-floored, rimless craters (40 km). In order to model further the amount of erosion based on the entire crater population, the shallowest slopes of the modelled curves (Figure 13) were set equal to the slope of the curve for the entire population of craters in the cratered highland materials (−1.29; Figure 5). This allows the depth of erosion to be determined relative to the decrease in crater diameter and compared to the data observed in the Amenthes and Tyrrhena region.

Based on the modelled curves (Figure 13) and the interior slopes of the craters, a 20-km-diameter event would erode a 10-km crater to a diameter of only 3.6 km resulting from the erosion of 995 m of material. The actual depth of erosion is difficult to determine because a large population of pristine craters covering a wide range of diameters does not exist on Mars, making a true production curve impossible to derive. In order to get slopes on the modelled curves equal to the actual slopes of the curves for the rimless crater population, slightly more than 1.4 km of material would have to be eroded.

Discussion

Based on the morphology of the Amenthes/Tyrrhena surface, the age relations determined by the crater frequency distributions, and analysis of likely resurfacing mechanisms, we believe that an erosive mechanism is a more likely explanation for the population of rimless craters than simple deposition up to the rims of an old crater population. The modelled curves illustrate what happens to a crater population that has undergone a purely erosional event. As a result, the curves for the larger diameter events take into account the removal of smaller craters (Figure 13). However, smaller rimless craters are obviously being preserved to some extent (Figures 3 and 4). Thus material eroded from large craters must be simultaneously deposited on top of the rimless smaller craters in order to preserve them. If such erosion and deposition were operating at the same intensity in the cratered plateau and cratered highland materials, their crater curves would be identical. The fact that the curves cross over at 16 km suggests that in part, the modelled erosional process operated at the same intensity with respect to the larger craters. Craters <16-km-diameter were either preferentially eroded from the cratered highlands, or the population of small craters in the cratered plateau materials were buried and have since been exhumed. Evidence for exhumation (Figure 14) is present in the highlands to the east and in the highland materials of the Ismenius Lacus quadrangle (A. M. Dimitriou, personal communication, 1989). Exhumation also explains the differences in geologic units: Cratered plateau material does not contain the same density of ancient valley networks as the cratered highlands, nor does it have the etched appearance on the surface separating craters. This suggests that as much as 1 km of erosion has removed the valley networks from the cratered plateau materials, exposing the buried small craters.

Erosion of the highlands to depths of 500–1500 m provides the material needed to bury smaller craters. The curves for

TABLE 2*b*. Crater Frequencies From *Neukum* [1983] and Associated Volumes

Diameter, km	Frequency From *Neukum* [1983]	Volume, km^3	Cumulative Volumes, km^3
2.0	10,500	10,238	10,238
5.0	2,200	42,174	52,412
10.0	900	104,004	156,416
20.0	320	129,856	286,272
30.0	180	198,916	485,188
40.0	70	157,451	642,639
50.0	28	109,026	751,665

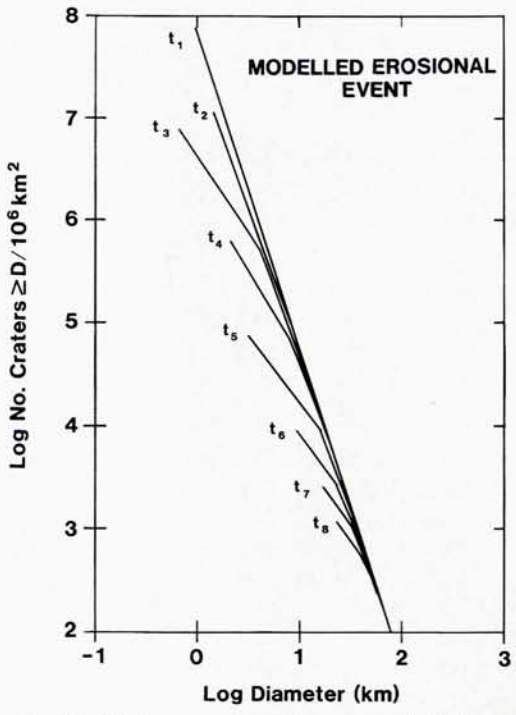

Fig. 13. Modelled crater curves for progressively larger diameter erosional events. Curve at t_1 is the modelled production curve extrapolated from *Neukum* [1983] for smaller (<30 km) diameter craters. Curve at t_2 represents a 2-km erosional event, t_3 is 5-km erosional event, t_4 is a 10-km erosional event, and t_5 through t_8 represent 20–50 km events at 10-km intervals. A 50-km event matches the total crater population curves for the cratered plateau (Figure 4) and the cratered highland materials (Figure 5).

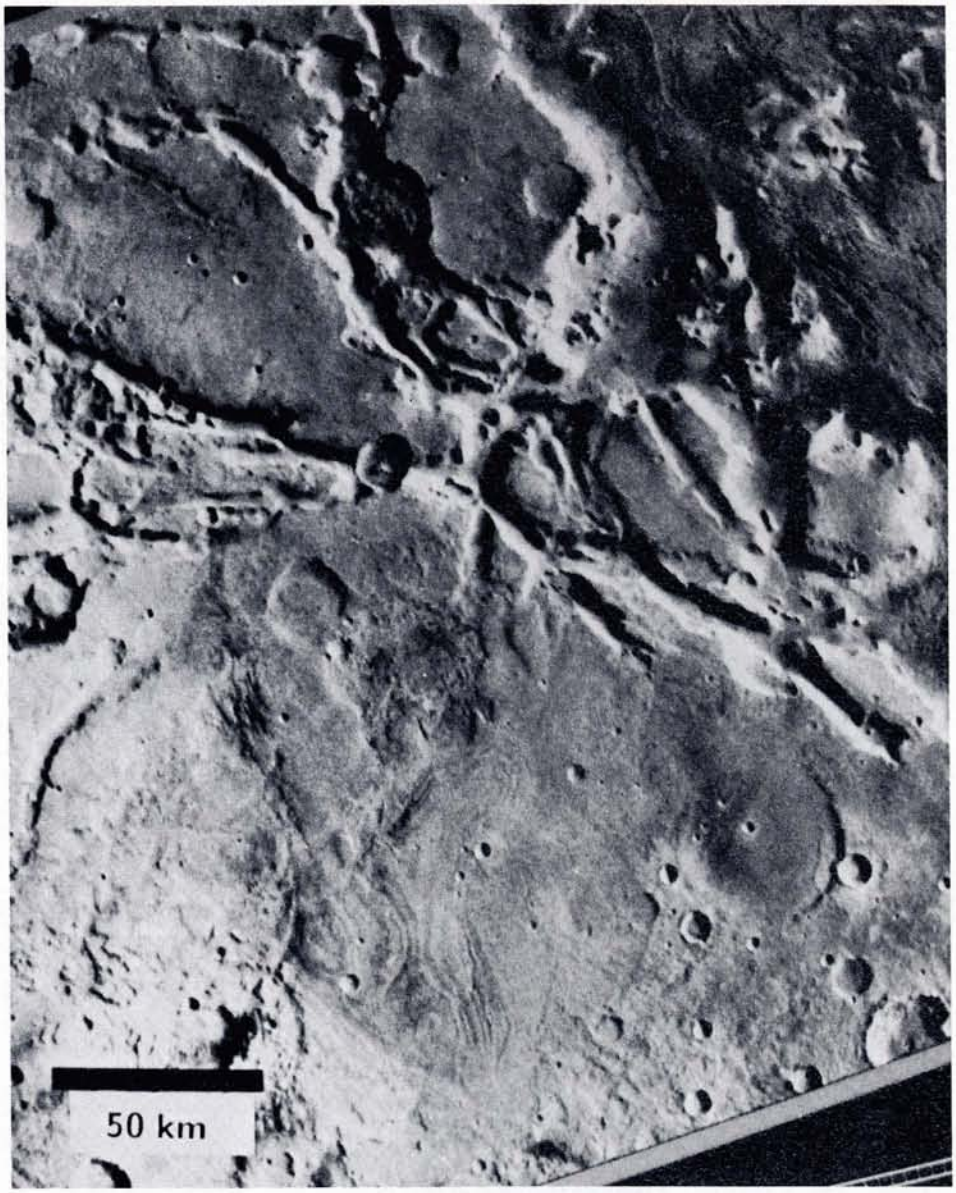

Fig. 14*a*. Evidence for late stage (aeolian?) erosion in the region surrounding Amenthes/Tyrrhena. Stripped layers in the Aeolis quadrangle (MC-23) of Mars, directly east of the Amenthes quadrangle. (Viking orbiter frame 631A27.)

the cratered plateau material separated into 5° latitude bins (Figure 6) indicate that the area near the boundary became stable first followed by successive southerly areas upslope from the boundary. The overall slope in the region is between 3 and 8 m/km (topography from the *U.S. Geological Survey* [1989]), sufficient to allow transport of eroded highland material to the edge of the boundary as well as local depositional centers. With time, depositional centers migrated to progressively southerly latitudes. Additional work by *Dimitriou* [1989] suggests that this resurfacing event and the associated age relationships between highland and near-boundary materials are widespread.

Large volumes of material may have been transported to great distances as well. *Grizzaffi and Schultz* [1989] have suggested that small, curvilinear ridges and mounds in the Isidis basin are the result of an air fall deposit which was interlain with ice and was subsequently eroded by the wind. The timing of this resurfacing event is $N(5) = 240$ [*Grizzaffi and Schultz*, 1989, Figure 11], corresponding well with the timing of resurfacing in the cratered highland and cratered plateau materials ($N(5) = 200$ and 250, respectively). The ancient volatile-rich debris layer in Isidis may represent an indirect result of extensive highland erosion which ceased during the late Noachian to early Hesperian. Even farther transport may be present as sedimentary material deposited in the northern plains [*McGill*, 1986]. A large depressed area west of Elysium is characterized by giant polygons, best explained as the locus of deposition of material eroded from surrounding regions.

CONCLUSIONS

1. Resurfacing terminated in the Amenthes and Tyrrhena region at $N(5) = 200$–250 (late Noachian to early Hesperian).

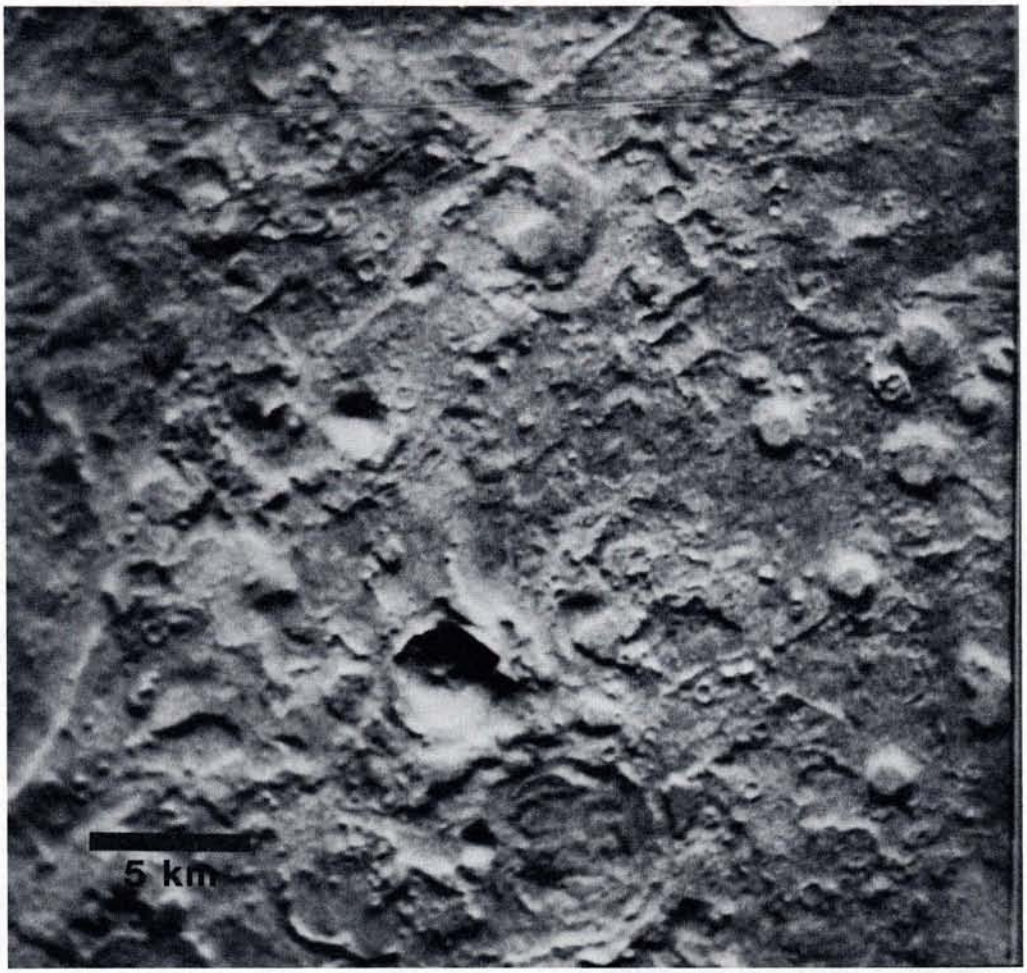

Fig. 14*b*. Inverted craters in the Syrtis Major quadrangle (MC-13), northwest of the Amenthes/Tyrrhena region. (Viking orbiter frame 678A08.) North is at the top.

Cumulative size-frequency distribution curves suggest that material near the dichotomy boundary became stable first followed by increasing southerly latitudes.

2. Aeolian and volcanic depositional processes do not explain the morphology of modified craters observed in the Martian highlands, nor do these processes explain fluctuations in the cumulative crater size-frequency distribution curves. Erosive processes capable of eroding the rims of craters and the surrounding material and simultaneously burying smaller craters explains both sets of observations.

3. Models of erosion suggest that between 500 m and 1.5 km of material was stripped from the highlands. Some eroded material remained locally, burying small impact craters before their complete eradication. Additional eroded material may have been transported to areas such as the Isidis basin and into low areas of the northern plains. Subsequent removal of the highlands deposits by aeolian processes (which may still be operating) is evident not only in the cratered plateau materials of the Amenthes and Tyrrhena region but also in the Isidis basin and in the Ismenius Lacus region. Exhumation of craters <16 km in diameter may explain the apparent age difference between the cratered plateau and cratered highland materials ($N(5) = 790$ versus $N(5) = 540$, respectively).

Future experimental and quantitative modelling of the different resurfacing processes will allow more accurate determinations of the importance of each process in Martian history with special emphasis on the Martian highlands. The timing and extent of each process will be important for understanding the evolution of the Martian crust, the atmosphere, and the volatile inventory.

Acknowledgments. We have benefitted from discussions with Andy Dimitriou, Herb Frey, George McGill, Rick Schultz, Tom Watters, and Jim Zimbelman, whose experimental data were very useful in understanding the aeolian resurfacing process. We thank Pete Schultz and Dave Scott for their thorough reviews of this manuscript. Beatrice Matkovic and Carolyn Russo aided in figure preparation. This research was supported by NASA grant NAGW-129.

REFERENCES

Baker, V. R., and D. J. Milton, Erosion by catastrophic floods on Mars and Earth, *Icarus*, *23*, 27–41, 1974.

Carr, M. H., H. Masursky, and R. S. Saunders, A generalized geologic map of Mars, *J. Geophys. Res.*, *78*, 4031–4036, 1973.

Carr, M. H., L. S. Crumpler, J. A. Cutts, R. Greeley, J. E. Guest, and H. Masursky, Martian impact craters and emplacement of ejecta by surface flow, *J. Geophys. Res.*, *82*, 4055–4065, 1977.

Chapman, C. R., and K. L. Jones, Cratering and obliteration history of Mars, *Annu. Rev. Earth Planet. Sci.*, *5*, 515–540, 1977.

Craddock, R. A., and T. A. Maxwell, Timing of resurfacing events in the Amenthes and Tyrrhena cratered highlands of Mars (abstract), *Lunar Planet. Sci., XX*, 191–192, 1989.

Cruikshank, D. P., W. K. Hartmann, and C. A. Wood, Moon: "Ghost" craters formed during mare filling, *Moon*, *7*, 440–452, 1973.

Dimitriou, A. M., Geologic evolution of the highland/lowland transition zone in the Ismenius Lacus quadrangle, Mars (abstract), *Lunar Planet. Sci., XX*, 246–247, 1989.

Frey, H. V., and T. Grant, Resurfacing in Coprates and thickness of the ridged plains (abstract), *Lunar Planet. Sci., XX*, 313–314, 1989.

Frey, H. V., A. M. Semeniuk, J. A. Semeniuk, and S. Tokarcik, A widespread common age resurfacing event in the highland-lowland transition zone in eastern Mars, *Proc. Lunar. Planet. Conf., 18th*, 679–699, 1988*a*.

Frey, H. V., J. A. Semeniuk, and T. Grant, Early resurfacing events on Mars (abstract), in *Abstracts for the MEVTV-LPI Workshop: Early Tectonic and Volcanic Evolution of Mars*, pp. 24–26, Lunar and Planetary Institute, Houston, Tex., 1988*b*.

Greeley, R., and J. E. Guest, Geologic map of the eastern hemisphere of Mars, scale 1:15M, *U.S. Geol. Surv. Misc. Invest. Ser. Map, I-1802-B*, 1987.

Greeley, R., and P. D. Spudis, Volcanism on Mars, *Rev. Geophys., 19*, 13–41, 1981.

Grizzaffi, P., and P. H. Schultz, Isidis basin: Site of ancient volatile-rich debris layer, *Icarus*, *77*, 358–381, 1989.

Hartmann, W. K., Martian cratering, III, Theory of crater obliteration, *Icarus*, *15*, 410–428, 1971.

Hartmann, W. K., Martian cratering 4: Mariner 9 initial analysis of cratering chronology, *J. Geophys. Res.*, *78*, 4096–4116, 1973.

Hartmann, W. K., R. G. Strom, S. J. Weidenschilling, K. R. Blasius, A. Woronov, M. R. Dence, R. A. F. Grieve, J. Diaz, C. R. Chapman, E. M. Shoemaker, and K. L. Jones, Chronology of planetary volcanism by comparative studies of planetary cratering, in *Basaltic Volcanism on the Terrestrial Planets*, pp. 1049–1127, Pergamon, New York, 1981.

Klein, S. P., and B. R. White, Dynamic shear of granular material under variable gravity conditions, *Rep. AIAA-88-0648*, 10 pp., Am. Assoc. of Aeronaut. and Astronaut., Washington, D. C., 1988.

Leighton, R. B., B. C. Murray, R. P. Sharp, J. D. Allen, and R. K. Sloan, Mariner IV photography of Mars: Initial results, *Science*, *149*, 627–630, 1965.

Lucchitta, B. K., H. M. Ferguson, and C. Summers, Sedimentary deposits in the northern lowland-plains, Mars, *Proc. Lunar Planet. Sci. Conf. 17th*, Part 1, *J. Geophys. Res.*, *91*, suppl., E166–E174, 1986.

Masursky, H., An overview of geologic results from Mariner 9, *J. Geophys. Res.*, *78*, 4009–4030, 1973.

Masursky, H., J. M. Boyce, A. L. Dial, G. G. Schaber, and M. E. Strobell, Classification and time formation of Martian channels based on Viking data, *J. Geophys. Res.*, *82*, 4016–4038, 1977.

Maxwell, T. A., and G. E. McGill, Ages of fracturing and resurfacing in the Amenthes region, Mars, *Proc. Lunar Planet. Sci. Conf., 18th*, 701–711, 1988.

McGill, G. E., The giant polygons of Utopia, northern Martian plains, *Geophys. Res. Lett.*, *13*, 705–708, 1986.

McGill, G. E., Relative age of faulting, mesa development, and polygonal terrane, eastern Utopia Planitia, Mars (abstract), *Lunar Planet. Sci., XVIII*, 620–621, 1987.

Milton, D. J., Water processes of degradation in the Martian landscape, *J. Geophys. Res.*, *78*, 4037–4047, 1973.

Moore, J. M., Nature of the mantling deposit in the heavily cratered terrain of northeastern Arabia, Mars, *J. Geophys. Res.*, this issue.

Murray, B. C., L. A. Soderblom, R. P. Sharp, and J. A. Cutts, The surface of Mars, I, Cratered terrains, *J. Geophys. Res.*, *76*, 313–330, 1971.

Neukum, G., *Meteoritenbombardment und Daitierung Planetarer Oberflachen, Habilitationsschrift*, 186 pp., Ludwig-Maximilians-Universität, Munich, 1983.

Neukum, G., and K. Hiller, Martian ages, *J. Geophys. Res.*, *86*, 3097–3121, 1981.

Neukum, G., and D. U. Wise, Mars: A standard crater curve and possible new time scale, *Science*, *194*, 1381–1387, 1976.

Opik, E. J., The Martian surface, *Science*, *153*, 255–265, 1966.

Pieri, D., Distribution of small channels on the Martian surface, *Icarus*, *27*, 25–50, 1976.

Pieri, D., Martian valleys: Morphology, distribution, age, and origin, *Science*, *210*, 895–897, 1980.

Pike, R. J., and P. A. Davis, Toward a topographic model of Martian craters from photoclinometry (abstract), *Lunar Planet. Sci., XV*, 645–646, 1984.

Plescia, J. B., and M. P. Golombek, Origin of planetary wrinkle ridges based on the study of terrestrial analogs, *Geol. Soc. Am. Bull.*, *97*, 1289–1299, 1986.

Scott, D. H., and M. H. Carr, Geologic map of Mars, scale 1:25M, *U.S. Geol. Surv. Misc. Invest. Ser. Map, I-1083*, 1978.

Scott, D. H., and K. L. Tanaka, Geologic map of the western hemisphere of Mars, *U.S. Geol. Surv. Misc. Invest. Ser. Map, I-1802-A*, 1986.

Sharp, R. P., Mars: Troughed terrain, *J. Geophys. Res.*, *78*, 4063–4083, 1973.

Sharp, R. P., and M. C. Malin, Channels on Mars, *Geol. Soc. Am. Bull.*, *86*, 593–609, 1975.

Soderblom, L. A., M. C. Malin, J. A. Cutts, and B. C. Murray, Mariner 9 observations of the surface of Mars in the north polar region, *J. Geophys. Res.*, *78*, 4197–4210, 1973.

Squyres, S. W., Urey prize lecture: Water on Mars, *Icarus*, *79*, 229–288, 1989.

Squyres, S. W., and M. H. Carr, Geomorphic evidence for the distribution of ground ice on Mars, *Science*, *231*, 249–252, 1986.

Tanaka, K. L., The stratigraphy of Mars, *Proc. Lunar Planet. Sci. Conf. 17th*, Part 1, *J. Geophys. Res.*, *91*, suppl., E139–E158, 1986.

Tanaka, K. L., N. K. Isbell, D. H. Scott, R. Greeley, and J. E. Guest, The resurfacing history of Mars: A synthesis of digitized, Viking-based geology, *Proc. Lunar Planet. Sci.*, *18*, 665–678, 1988.

U.S. Geological Survey, Shaded relief map of Mars, scale 1:15M, *U.S. Geol. Surv. Misc. Invest. Ser. Map, I-1618*, 1985.

U.S. Geological Survey, Topographic maps of the western, eastern equatorial and polar regions of Mars, scale 1:15M, *U.S. Geol. Surv. Misc. Invest. Ser. Map, I-2030*, 1989.

Watters, T. R., Wrinkle ridge assemblages on the terrestrial planets, *J. Geophys. Res.*, *93*, 236–254, 1988.

Watters, T. R., and T. A. Maxwell, Crosscutting relations and relative ages of ridges and faults in the Tharsis region of Mars, *Icarus*, *56*, 278–298, 1983.

Watters, T. R., and T. A. Maxwell, Orientation, relative age, and extent of the Tharsis Plateau ridge system, *J. Geophys. Res.*, *91*, 8113–8125, 1986.

Wilhelms, D. E., and R. J. Baldwin, The role of igneous sills in shaping the Martian uplands, *Proc. Lunar Planet. Sci., 19th*, 355–365, 1989.

Wise, D. U., M. P. Golombek, and G. E. McGill, Tectonic evolution of Mars, *J. Geophys. Res.*, *84*, 7934–7939, 1979.

Wood, C. A., and L. Andersson, New morphometric data for fresh lunar craters, *Proc. Lunar Planet. Sci. Conf.*, *9*, 3669–3689, 1978.

Zimbelman, J. R., and R. Greeley, Simulated mantled surfaces on cratered terrain (abstract), *Lunar Planet. Sci., XII*, 1233–1235, 1981.

R. A. Craddock and T. A. Maxwell, Center for Earth and Planetary Studies, National Air and Space Museum, Smithsonian Institution, Washington, DC 20560.

(Received July 5, 1989;
revised March 30, 1990;
accepted April 5, 1990.)